Int. J. Solids Structures Vol. 27, No. 14, pp. 1809–1828, 1991
Printed in Great Britain.

0020-7683/91 $3.00 + .00

BUCKLING INSTABILITIES IN A THICK ELASTIC THREE-PLY COMPOSITE PLATE UNDER THRUST

THOMAS J. PENCE and JOHN SONG
Department of Metallurgy, Mechanics and Material Science, Michigan State University, East Lansing, MI 48824-1226, U.S.A.

(*Received* 14 *October* 1989; *in revised form* 10 *August* 1990)

Abstract—The buckling of a three-ply sandwich composite plate is studied in the context of finite deformation incompressible nonlinear elasticity. As is the case of a noncomposite plate, buckled configurations involving either barrelling or flexure are possible. However, the ordering of the failure thrusts for certain composite configurations is more complicated than the ordering that occurs in the noncomposite case. In particular, under suitable conditions, the thrusts at which barrelling and flexural buckling modes occur can be interlaced. Furthermore, transitions in the ordering of the different failure modes may occur as the aspect ratio of the plate is varied.

1. INTRODUCTION

We consider the buckling of a composite plate composed of three stacked rectangular plies with perfect interfacial bonding and subjected to a total end thrust T. The end plies are identical both in thickness and material. The geometry and loading of a particular plate configuration is depicted in Fig. 1. The problem is studied in the context of finite deformation incompressible nonlinear elasticity. All three plies consist of neo-Hookean materials, so that for given external dimensions l_1, l_2 and l_3, the composite construction is characterized by two parameters: (i) β, which is the ratio of the stiffness of the inner material to the outer material, and (ii) α, which is the volume fraction of the central ply within the complete construction. The three special cases of $\beta = 1$, $\alpha = 0$ or $\alpha = 1$ correspond to a homogeneous, isotropic (noncomposite) plate which has been extensively studied by Sawyers and Rivlin (1974, 1982). Our purpose is to consider the effect that composite construction has on buckling instability failure. Sawyers and Rivlin (1974, 1982) have shown for the noncomposite case that buckling can occur in the (X_1, X_2)-plane involving either flexural or barrelled mode shapes with an arbitrary integer number m of half-wavelengths. A diagram

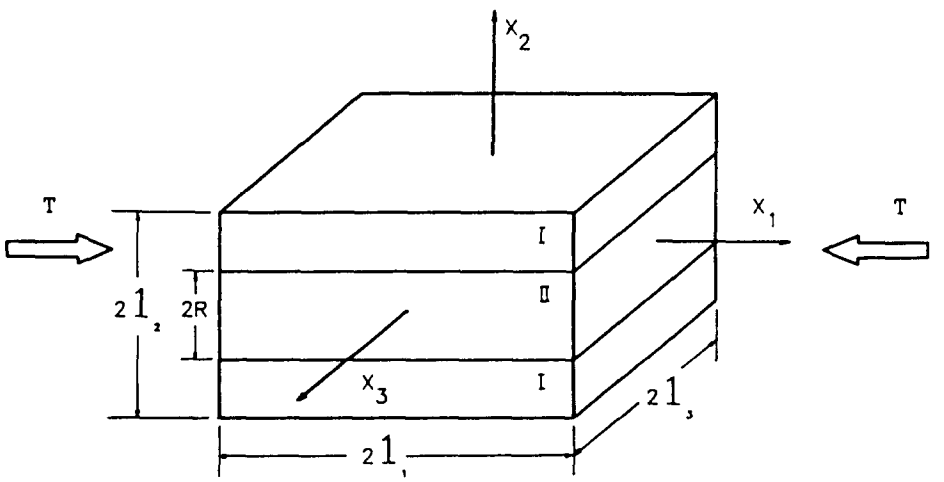

Fig. 1. Geometry of the composite plate under consideration. The buckled configurations of interest involve deformations in the (X_1, X_2)-plane.

of these failure modes, as they would occur in the composite construction under consideration here, is presented in Fig. 2, where T_m^F and T_m^B ($m = 1, 2, 3, \ldots$) denote the corresponding failure thrusts. Of particular interest is the ordering of these failure thrusts. Sawyers and Rivlin (1974, 1982) have shown that for the noncomposite case these thrusts are always ordered as follows:

$$0 < T_1^F < T_2^F < \cdots < T_m^F < T_{m+1}^F < \cdots \rightarrow T_\infty \leftarrow \cdots < T_{m+1}^B < T_m^B < \cdots < T_2^B < T_1^B. \tag{1}$$

Here T_∞ is the value associated with an infinite number of wavelengths and can be identified with a wrinkling instability.

For the composite construction we obtain some striking differences. Most notable is that, under suitable conditions, the failure thrusts cease to be ordered as in (1). We demonstrate that the following two results, neither of which occur in the noncomposite case, may, under suitable conditions, take place for a three-ply composite construction: (i) an interlacing of the thrusts at which barrelling and flexural buckling occur, and (ii) the occurrence of the lowest—or critical—failure mode corresponding to a mode other than $m = 1$ flexure. In fact the critical buckling instability is often found to be the wrinkling instability corresponding to $m = \infty$. In such cases, for fixed values of β and α, the critical instability is governed by the aspect ratio l_2/l_1. In fact, it is shown that there is a transition between critical instabilities which is aspect ratio dependent. Such a transition in critical instabilities for a noncomposite plate is of course not possible, since in such a case (1) always holds. It is interesting to note however that a different but similar transition in critical instabilities has been shown to exist by Simpson and Spector (1984) in certain types of noncomposite *column* buckling. A thorough discussion of recent results concerning buckling instabilities in *homogeneous* elastic solids has recently been given by Davies (1989).

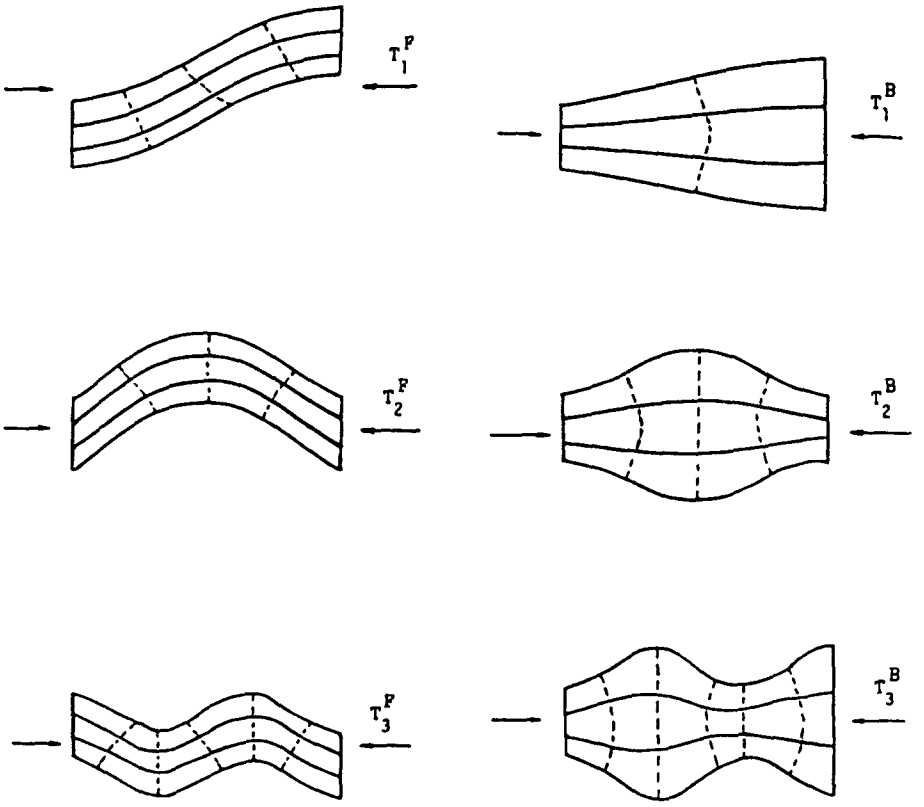

Fig. 2. Examples of the flexural and barrelling buckling modes, and failure thrusts, for $m = 1, 2$ and 3. Higher order buckling modes involve a repetition of the basic $m = 1$ half-wavelength mode shape.

along with rigorous results concerning the relation between buckling instabilities and energy minimization for a problem involving a homogeneous compressible elastic solid. Finally, it is to be noted that drastic changes in stability type for composite construction have recently been demonstrated by Horgan and Pence (1989) for the void formation instability mechanism.

2. PROBLEM DESCRIPTION

We consider a thick rectangular plate occupying the region $-l_i \leqslant X_i \leqslant l_i$ $(i = 1, 2, 3)$ before the application of loads. The plate is constructed from three plies that are stacked symmetrically as follows:

$$\begin{aligned} &\text{ply 1:} \quad -l_2 < X_2 < -R, \\ &\text{ply 2:} \quad -R < X_2 < R, \\ &\text{ply 3:} \quad R < X_2 < l_2. \end{aligned} \tag{2}$$

Plies 1 and 3 are taken to consist of the same incompressible, isotropic, homogeneous elastic material (material I). Ply 2 is also composed of an incompressible, isotropic, homogeneous material (material II) which is in general different from material I.

Within each ply we define a deformation

$$\mathbf{x} = \mathbf{x}(\mathbf{X}), \tag{3}$$

with deformation gradient tensor

$$\mathbf{F} = \partial \mathbf{x}/\partial \mathbf{X}. \tag{4}$$

The requirement of material incompressibility is that

$$\det \mathbf{F} = 1. \tag{5}$$

The Cauchy stress tensor is then given by

$$\tau = -p\mathbf{I} + 2(\partial W/\partial I_1 + I_1 \partial W/\partial I_2)\mathbf{B} - 2(\partial W/\partial I_2)\mathbf{B}^2. \tag{6}$$

Here p is hydrostatic pressure, $\mathbf{B} = \mathbf{F}\mathbf{F}^{\mathrm{T}}$ is Green's deformation tensor, I_1, I_2 are the first and second invariants of $\mathbf{B}$, and W is the strain energy density function of the material,

$$W = \begin{cases} W^{\mathrm{I}}(I_1, I_2), & \text{in plies 1 and 3,} \\ W^{\mathrm{II}}(I_1, I_2), & \text{in ply 2.} \end{cases}$$

The Piola–Kirchoff stress tensor is then given by

$$\mathbf{S} = \mathbf{F}^{-1}\tau, \tag{7}$$

and the equilibrium equations are

$$\operatorname{div} \mathbf{S}^{\mathrm{T}} = 0. \tag{8}$$

The plate is subjected to a thrust on each of the surfaces $X_1 = \pm l_1$. We consider the specific boundary conditions:

$$S_{12} = S_{13} = 0, \quad \text{on } X_1 = \pm l_1, \tag{9}$$

$$x_1 = \pm \rho l_1, \quad \text{on } X_1 = \pm l_1, \tag{10}$$

corresponding to a frictionless thrust with an overall stretch ratio of ρ. We shall regard $\rho > 0$, rather than the thrust, as a prescribed constant. The physically interesting case of compression corresponds to $0 < \rho < 1$.

The surfaces $X_2 = \pm l_2$ are assumed to be traction free so that the following boundary conditions are required to hold:

$$S_{21} = S_{22} = S_{23} = 0, \quad \text{on } X_2 = \pm l_2. \tag{11}$$

On the surfaces $X_3 = \pm l_3$, the following boundary conditions are required to hold:

$$S_{31} = S_{32} = 0, \quad \text{on } X_3 = \pm l_3, \tag{12}$$

$$x_3 = \pm l_3, \quad \text{on } X_3 = \pm l_3, \tag{13}$$

corresponding to a frictionless clamp. Problems of this type for homogeneous (non-composite) plates have been studied by Sawyers and Rivlin (1974, 1982).

In order to treat the composite three-ply laminate, the additional interface conditions are required to hold:

$$S_{2i}|_{X_2^+} = S_{2i}|_{X_2^-} \quad (i = 1, 2, 3), \quad X_2 = \pm R, \tag{14}$$

$$\mathbf{x}|_{X_2^+} = \mathbf{x}|_{X_2^-}, \quad X_2 = \pm R. \tag{15}$$

Conditions (14) and (15) correspond to a case in which the plies are perfectly bonded across the interfaces.

We shall henceforth restrict our attention to the case in which both material I and material II are neo-Hookean with shear moduli $\mu^{(I)}$ and $\mu^{(II)}$, respectively. Thus

$$W^{I} = \mu^{(I)}(I_1 - 3)/2, \quad W^{II} = \mu^{(II)}(I_1 - 3)/2, \tag{16}$$

so that (6) yields:

$$\tau = -p\mathbf{I} + \mu^{(j)}\mathbf{B}, \quad j = \mathrm{I}, \mathrm{II}. \tag{17}$$

To within an arbitrary displacement in the X_2-direction, there is exactly one pure homogeneous deformation solution to the foregoing boundary value problem. The underlying deformation must be given by

$$\begin{aligned} x_1 &= \rho X_1, \\ x_2 &= \rho^{-1} X_2, \\ x_3 &= X_3, \end{aligned} \tag{18}$$

in order to satisfy (10), (13) and (5). Thus the principal stretches $\lambda_1, \lambda_2, \lambda_3$ are given by $\lambda_1 = \rho$, $\lambda_2 = \rho^{-1}$, $\lambda_3 = 1$. The material deformation tensor $\mathbf{F}$ and Green's deformation tensor $\mathbf{B}$ are in this case given by

$$\mathbf{F} = \mathrm{diag}\,(\rho, \rho^{-1}, 1), \quad \mathbf{B} = \mathrm{diag}\,(\rho^2, \rho^{-2}, 1). \tag{19}$$

Both the Cauchy stress tensor (17) and the Piola–Kirchoff stress tensor (7) are constant

in each ply so that (8) is automatically satisfied. Now the conditions $(11)_2$ and $(14)_{i=2}$ in conjunction with (17), (7), (19) give

$$p = \mu^{(j)}\rho^{-2} \equiv p^{(j)}, \quad j = \text{I, II}. \tag{20}$$

Therefore

$$\tau = \mu^{(j)}\begin{bmatrix} \rho^2-\rho^{-2} & & \\ & 0 & \\ & & 1-\rho^{-2} \end{bmatrix} \equiv \tau^{(j)}, \quad j = \text{I, II}, \tag{21}$$

and

$$\mathbf{S} = \mu^{(j)}\begin{bmatrix} \rho-\rho^{-3} & & \\ & 0 & \\ & & 1-\rho^{-2} \end{bmatrix} \equiv \mathbf{S}^{(j)}, \quad j = \text{I, II}. \tag{22}$$

Note that the remaining conditions (9), (11), (12) and (14) are automatically satisfied.

Let Q be the total load applied to each of the faces $X_1 = \pm l_1$. Then

$$Q = Q^{(\text{I})} + Q^{(\text{II})}, \tag{23}$$

where $Q^{(j)}$ ($j = \text{I, II}$) is the load applied to material j. Thus for the homogeneous solution

$$\tau_{11}^{(j)} = Q^{(j)}/A^{(j)}, \tag{24}$$

where $A^{(j)}$ ($j = \text{I, II}$) is the current area of the surface to which $Q^{(j)}$ is applied,

$$A^{(\text{I})} = 4(l_2 - R)l_3\rho^{-1}, \quad A^{(\text{II})} = 4Rl_3\rho^{-1}. \tag{25}$$

Using (21)-(25), it is found that

$$Q^{(\text{I})} = \frac{(l_2 - R)\mu^{(\text{I})}}{R\mu^{(\text{II})} + (l_2 - R)\mu^{(\text{I})}}\, Q, \tag{26}$$

$$Q^{(\text{II})} = \frac{R\mu^{(\text{II})}}{R\mu^{(\text{II})} + (l_2 - R)\mu^{(\text{I})}}\, Q, \tag{27}$$

$$Q = 4l_3(\rho - \rho^{-3})[R\mu^{(\text{II})} + (l_2 - R)\mu^{(\text{I})}]. \tag{28}$$

Note that Q is monotone increasing in ρ from $Q = -\infty$ when $\rho = 0$ to $Q = \infty$ when $\rho = \infty$, with $Q = 0$ when $\rho = 1$. The thrust T on the end faces is then given by

$$T = -Q. \tag{29}$$

3. BIFURCATION FROM THE HOMOGENEOUS SOLUTION

We now investigate the stability of the homogeneous deformation solution given above. Following Sawyers and Rivlin (1974, 1982), we shall restrict our attention to the case where buckling takes place in the (X_1, X_2)-plane. To do so, we consider the fully finite deformation

$$\begin{aligned} \hat{x}_1 &= \rho X_1 + \varepsilon\bar{u}_1(X_1, X_2), \\ \hat{x}_2 &= \rho^{-1}X_2 + \varepsilon\bar{u}_2(X_1, X_2), \\ \hat{x}_3 &= X_3, \end{aligned} \tag{30}$$

where $\bar{u}_1$, $\bar{u}_2$ are unknown functions which are independent of X_3 by assumption. In this section we shall use a superposed $\hat{}$ to indicate quantities associated with the finite deformation (30). Here ε is an order parameter which is introduced for the purposes of obtaining a linearized problem governing bifurcation from the homogeneous deformation solution (18). Finally, a superposed $\bar{}$ will be used to indicate the $O(\varepsilon)$ difference between quantities associated with $\hat{x}$ and quantities associated with this homogeneous deformation solution. Thus, for example, the pressure field corresponding to (30) will be given by

$$\hat{p}(\mathbf{X}, \varepsilon) = p^{(j)} + \varepsilon \bar{p}(X_1, X_2, X_3) + O(\varepsilon^2), \quad j = \mathrm{I}, \mathrm{II}, \tag{31}$$

and the Piola–Kirchoff stress tensor is given by

$$\hat{\mathbf{S}}(\mathbf{X}, \varepsilon) = \mathbf{S}^{(j)} + \varepsilon \bar{\mathbf{S}}(X_1, X_2, X_3) + \mathbf{O}(\varepsilon^2), \quad j = \mathrm{I}, \mathrm{II}. \tag{32}$$

The material deformation tensor associated with (30) is given by

$$\hat{\mathbf{F}} = \begin{bmatrix} \rho + \varepsilon \bar{u}_{1,1} & \varepsilon \bar{u}_{1,2} & 0 \\ \varepsilon \bar{u}_{2,1} & \rho^{-1} + \varepsilon \bar{u}_{2,2} & 0 \\ 0 & 0 & 1 \end{bmatrix}, \tag{33}$$

so that

$$\det \hat{\mathbf{F}} = [1 + \varepsilon(\rho \bar{u}_{2,2} + \rho^{-1} \bar{u}_{1,1}) + \varepsilon^2 (\bar{u}_{1,1} \bar{u}_{2,2} - \bar{u}_{1,2} \bar{u}_{2,1})]. \tag{34}$$

It is well known that the solution to the corresponding linearized boundary value problem locates the failure thrusts at which bifurcation occurs from a homogeneous solution of the type (18) [see Davies (1989) for a rigorous discussion of a problem involving a noncomposite compressible elastic material]. An analysis of the linear problem will not reveal the details of the post-buckling and moreover may underestimate the actual thrusts at which instability occurs for the case of snap-buckling. These more difficult issues will not be treated in this communication. Rather we shall in this paper concern ourselves with determining the failure thrusts at which bifurcation takes place locally from the homogeneous solution (18). Thus it follows from (5), (34) that the linearized problem governing local bifurcation obeys

$$\rho^{-2} \bar{u}_{1,1} + \bar{u}_{2,2} = 0. \tag{35}$$

One obtains from (33), (35)

$$\hat{\mathbf{B}} = \begin{bmatrix} \rho^2 + \varepsilon(2\rho \bar{u}_{1,1}) & \varepsilon(\rho \bar{u}_{2,1} + \rho^{-1} \bar{u}_{1,2}) & 0 \\ \varepsilon(\rho \bar{u}_{2,1} + \rho^{-1} \bar{u}_{1,2}) & \rho^{-2} + \varepsilon(2\rho^{-1} \bar{u}_{2,2}) & 0 \\ 0 & 0 & 1 \end{bmatrix} + \mathbf{O}(\varepsilon^2),$$

$$\hat{\mathbf{F}}^{-1} = \begin{bmatrix} \rho^{-1} + \varepsilon \bar{u}_{2,2} & -\varepsilon \bar{u}_{1,2} & 0 \\ -\varepsilon \bar{u}_{2,1} & \rho + \varepsilon \bar{u}_{1,1} & 0 \\ 0 & 0 & 1 \end{bmatrix} + \mathbf{O}(\varepsilon^2). \tag{36}$$

Entering (17), (7) with (36) and using (20), (31), (32) it is found that

$$\begin{aligned} \bar{S}_{11} &= -\rho^{-1} \bar{p} + \mu^{(j)} [2\bar{u}_{1,1} + (\rho^2 - \rho^{-2}) \bar{u}_{2,2}], \\ \bar{S}_{12} &= \mu^{(j)} (\rho^{-2} \bar{u}_{1,2} + \bar{u}_{2,1}), \\ \bar{S}_{21} &= \mu^{(j)} (\rho^{-2} \bar{u}_{2,1} + \bar{u}_{1,2}), \\ \bar{S}_{22} &= -\rho \bar{p} + 2\mu^{(j)} \bar{u}_{2,2}, \end{aligned}$$

$$\bar{S}_{33} = -\bar{p},$$
$$\bar{S}_{13} = \bar{S}_{23} = \bar{S}_{31} = \bar{S}_{32} = 0. \tag{37}$$

The equilibrium equation (8) in conjunction with (37) then yields the following system of partial differential equations for the linearized problem:

$$\begin{aligned} -\rho^{-1}\bar{p}_{,1} + \mu^{(j)}(2\bar{u}_{1,11} + \rho^2\bar{u}_{2,21} + \bar{u}_{1,22}) &= 0, \\ -\rho\bar{p}_{,2} + \mu^{(j)}(2\bar{u}_{2,22} + \rho^{-2}\bar{u}_{1,12} + \bar{u}_{2,11}) &= 0, \quad (j = \mathrm{I}, \mathrm{II}) \\ -\bar{p}_{,3} &= 0. \end{aligned} \tag{38}$$

Note that $(38)_3$ is satisfied if and only if

$$\bar{p}(X_1, X_2, X_3) = \bar{p}(X_1, X_2). \tag{39}$$

In addition, boundary conditions (12) and (13) are satisfied automatically for the linearized problem. Thus the linearized problem for local bifurcation from the homogeneous solution (18) is governed by field equations $(38)_{1,2}$ and (35) for functions $\bar{u}_1(X_1, X_2)$, $\bar{u}_2(X_1, X_2)$, $\bar{p}(X_1, X_2)$ subjected to boundary conditions that follow from (9)–(11), (14) and (15). Following Sawyers and Rivlin (1974, 1982), we may obtain solutions for this problem in the form

$$\bar{u}_1 = \left.\begin{matrix} -\sin(\Phi X_1) \\ \cos(\Psi X_1) \end{matrix}\right\} U_1(X_2), \quad \bar{u}_2 = \left.\begin{matrix} \cos(\Phi X_1) \\ \sin(\Psi X_1) \end{matrix}\right\} U_2(X_2), \quad \bar{p} = \left.\begin{matrix} \cos(\Phi X_1) \\ \sin(\Psi X_1) \end{matrix}\right\} P(X_2), \tag{40}$$

where the choice of $\Phi = k\pi/l_1$ $(k = 1, 2, 3, \ldots)$ and $\Psi = (j - 1/2)\pi/l_1$ $(j = 1, 2, 3, \ldots)$ results in the satisfaction of boundary conditions obtained from linearizing (9), (10). Let $\Omega = \Phi$ or Ψ accordingly as one considers either the upper or lower terms in (40). Thus $\Omega = m\pi/2l_1$, where $m = 2k$ for the upper terms and $m = 2j - 1$ for the lower terms. We shall refer to m as the mode number since it determines the number of repeating half-wavelengths in the X_1-direction of a basic deformation mode.

For both the upper and lower terms in (40) the field equations $(38)_{1,2}$ and (35) become ordinary differential equations:

$$\begin{aligned} U_1'' - \Omega^2 U_1 - [(\Omega\rho^{-1})/(\mu^{(j)})]P &= 0, \\ U_2'' - \Omega^2 U_2 - [\rho/(\mu^{(j)})]P' &= 0, \quad j = \mathrm{I}, \mathrm{II}, \\ -\rho^{-2}\Omega U_1 + U_2' &= 0. \end{aligned} \tag{41}$$

Here the superscript $'$ denotes differentiation with respect to X_2. The boundary and interface conditions (11), (14)–(15) can also be written in terms of $P(X_2)$, $U_1(X_2)$, $U_2(X_2)$.

We define a new stretch ratio $\lambda = \lambda_2/\lambda_1 = \rho^{-2}$. Note that $\lambda > 1$ when the ends are compressed $(0 < \rho < 1)$, and $\lambda < 1$ when the ends are extended $(\rho > 1)$. To solve (41), we reduce this set of equations to a single ordinary differential equation for U_2 alone. This is accomplished by first solving $(41)_1$, and $(41)_3$ for U_1 and P in terms of derivatives of U_2. Upon using these results in $(41)_2$ one obtains a single fourth order ordinary differential equation for U_2,

$$U_2'''' - (1 + \lambda^2)\Omega^2 U_2'' + \lambda^2\Omega^4 U_2 = 0. \tag{42}$$

In a similar fashion the boundary conditions (11), (14), (15) give rise to:

$$\left.\begin{aligned}&(\lambda\Omega)^2U_2(X_2)+U_2''(X_2)=0\\&(\lambda\Omega)^2(2+1/\lambda^2)U_2'(X_2)-U_2'''(X_2)=0\end{aligned}\right\}\quad\text{on } X_2=\pm l_2,$$

$$\left.\begin{aligned}&U_2(X_{2^+})=U_2(X_{2^-})\\&U_2'(X_{2^+})=U_2'(X_{2^-})\end{aligned}\right\}\quad\text{on } X_2=\pm R,$$

$$\left.\begin{aligned}&\mu^{(j)}[(\lambda\Omega)^2U_2(X_{2^+})+U_2''(X_{2^+})]\\&\quad=\mu^{(\hat{j})}[(\lambda\Omega)^2U_2(X_{2^-})+U_2''(X_{2^-})]\\&\mu^{(j)}[(2+1/\lambda^2)(\lambda\Omega)^2U_2'(X_{2^+})-U_2'''(X_{2^+})]\\&\quad=\mu^{(\hat{j})}[(2+1/\lambda^2)(\lambda\Omega)^2U_2'(X_{2^-})-U_2'''(X_{2^-})]\end{aligned}\right\}\quad\text{on } X_2=\pm R, \tag{43}$$

where $X_2=-R$ implies $j=\text{II}$, $\hat{j}=\text{I}$ and $X_2=R$ implies $j=\text{I}$, $\hat{j}=\text{II}$.

The general solution of (42) can be expressed as

$$U_2=L_1(X_2)\cosh(\Omega_1X_2)+L_2(X_2)\sinh(\Omega_1X_2)+M_1(X_2)\cosh(\Omega_2X_2)+M_2(X_2)\sinh(\Omega_2X_2), \tag{44}$$

where

$$\left.\begin{matrix}\Omega_1^2\\\Omega_2^2\end{matrix}\right\}=\Omega^2\{(1+\lambda^2)\pm[(1+\lambda^2)^2-4\lambda^2]^{1/2}\}/2=\begin{cases}\Omega^2,\\\lambda^2\Omega^2.\end{cases} \tag{45}$$

Here we have introduced the four step functions $L_n(X_2)$, $M_n(X_2)$ for $n=1$ or 2 as

$$L_n(X_2)=\begin{cases}L_n^{(1)},\\L_n^{(2)},\\L_n^{(3)},\end{cases}\quad M_n(X_2)=\begin{cases}M_n^{(1)}, & X_2\in(-l_2,-R),\\M_n^{(2)}, & X_2\in(-R,R),\\M_n^{(3)}, & X_2\in(R,l_2).\end{cases} \tag{46}$$

The boundary conditions (43) now give rise to a 12×12 linear system for the 12 unknown constants given by the Ls and Ms. This system shall be written as

$$\mathbf{J}_{12\times12}\mathbf{L}_{12\times1}=\mathbf{0}_{12\times1}, \tag{47}$$

where

$$\mathbf{L}=(M_1^{(1)},M_2^{(1)},L_1^{(1)},L_2^{(1)},M_1^{(2)},M_2^{(2)},L_1^{(2)},L_2^{(2)},M_1^{(3)},M_2^{(3)},L_1^{(3)},L_2^{(3)})^{\mathrm{T}}, \tag{48}$$

and $\mathbf{J}$ is a 12×12 matrix described further in (51). Bifurcation takes place provided that a nontrivial solution exists for (47). This in turn requires that

$$\det\mathbf{J}=0. \tag{49}$$

Equation (49) can now be regarded as an equation for those λs and hence those ρs, at which buckling can occur for a given value of the mode variable $\Omega=m\pi/2l_1$.

It is convenient to study (49) by first introducing the following dimensionless parameters

$$\eta=\Omega l_2=m\pi l_2/2l_1,\quad \beta=\mu^{(\text{II})}/\mu^{(\text{I})},\quad \alpha=R/l_2. \tag{50}$$

Then $\mathbf{J}$ can be written as

$$\mathbf{J} = \begin{bmatrix} \mathbf{J}_{11} & \mathbf{J}_{12} & \mathbf{J}_{13} \\ \mathbf{J}_{21} & \mathbf{J}_{22} & \mathbf{J}_{23} \\ \mathbf{J}_{31} & \mathbf{J}_{32} & \mathbf{J}_{33} \end{bmatrix}, \tag{51}$$

where $\mathbf{J}_{mn}$ are 4×4 submatrices whose entries are functions of the parameters η, β, α and λ. These submatrices are given in the Appendix. Thus (49) becomes an equation

$$\Psi(\lambda, \eta, \beta, \alpha) = 0, \tag{52}$$

relating the four dimensionless parameters describing the problem at hand: (a) $\lambda = \rho^{-2} = \lambda_2/\lambda_1$—the ratio of the principal stretches at which buckling occurs, which according to (28) is the *load parameter*, (b) η—which is the *mode number* of the buckled configuration scaled with respect to the aspect ratio l_2/l_1, (c) β—which is the *stiffness ratio* of the two composite materials comprising the construction, and (d) α—which is the *volume fraction* of the central ply within the complete construction. These quantities are restricted by their definitions to lie in the following intervals: $\lambda > 0, \eta > 0, \beta > 0, 0 \leqslant \alpha \leqslant 1$. Although η must take on discrete values determined by the aspect ratio l_2/l_1, it can be treated as a continuous variable for the purposes of analysis.

We shall call (52) the *general buckling* equation. We note that this problem ought to reduce to the noncomposite case for the following two special cases:

$$\left.\begin{array}{l} \text{(i) } \beta = 1, \text{ since then material I is identical to material II,} \\ \text{(ii) either } \alpha = 0 \text{ or } \alpha = 1, \text{ since then only one phase is present.} \end{array}\right\} \tag{53}$$

4. TWO SPECIAL DEFORMATION TYPES: FLEXURE AND BARRELLING

For the noncomposite case, it is shown by Sawyers and Rivlin (1974, 1982) that two deformation types are possible within the class of plane strain deformations (30) under consideration here, the first of which is a flexural deformation and the second of which is a barrelling deformation. Moreover, it is also shown that these two types exhaust all posssible plane strain solutions. For the composite case, both of these deformation types remain possible. However, analytical difficulties have so far prevented us from showing that these two types exhaust all of the possible plane strain solutions. Nevertheless, in what follows we limit our attention to these two deformation types.

A *flexural deformation* is one in which U_2 is an even function of X_2 so that U_1 is an odd function of X_2 by virtue of $(41)_3$. This requires that

$$(M_1^{(1)}, M_2^{(1)}, L_1^{(1)}, L_2^{(1)}) = (M_1^{(3)}, -M_2^{(3)}, L_1^{(3)}, -L_2^{(3)}), \quad M_2^{(2)} = L_2^{(2)} = 0, \tag{54}$$

so that system (47) reduces from the 12×12 system to the following 6×6 system:

$$\begin{bmatrix} 2\lambda C_2 & -2\lambda S_2 & \Lambda C_1 & -\Lambda S_1 & 0 & 0 \\ -\Lambda S_2 & \Lambda C_2 & -2S_1 & 2C_1 & 0 & 0 \\ -C_4 & S_4 & -C_3 & S_3 & C_4 & C_3 \\ \lambda S_4 & -\lambda C_4 & S_3 & -C_3 & -\lambda S_4 & -S_3 \\ -2\lambda C_4 & 2\lambda S_4 & -\Lambda C_3 & \Lambda S_3 & 2\lambda\beta C_4 & \Lambda\beta C_3 \\ \Lambda S_4 & -\Lambda C_4 & 2S_3 & -2C_3 & -\Lambda\beta S_4 & -2\beta S_3 \end{bmatrix} \begin{bmatrix} M_1^{(1)} \\ M_2^{(1)} \\ L_1^{(1)} \\ L_2^{(1)} \\ M_1^{(2)} \\ L_1^{(2)} \end{bmatrix} = \mathbf{0}_{6\times 1}, \tag{55}$$

where

$$\begin{aligned} &C_1 = \cosh(\eta), \quad C_2 = \cosh(\lambda\eta), \quad C_3 = \cosh(\eta\alpha), \quad C_4 = \cosh(\lambda\eta\alpha), \\ &S_1 = \sinh(\eta), \quad S_2 = \sinh(\lambda\eta), \quad S_3 = \sinh(\eta\alpha), \quad S_4 = \sinh(\lambda\eta\alpha), \\ &\Lambda = (\lambda + 1/\lambda). \end{aligned} \tag{56}$$

In place of equation (52) one then obtains a simpler *flexural buckling equation* found by setting the determinant of the matrix in (55) equal to zero. We shall write this relation as:

$$\Psi_F(\lambda, \eta, \beta, \alpha) = 0. \tag{57}$$

A *barrelling deformation* is one in which U_2 is an odd function of X_2 and U_1 is an even function of X_2. This requires that

$$(M_1^{(1)}, M_2^{(1)}, L_1^{(1)}, L_2^{(1)}) = (-M_1^{(3)}, M_2^{(3)}, -L_1^{(3)}, L_2^{(3)}), \quad M_1^{(2)} = L_1^{(2)} = 0, \tag{58}$$

which in turn gives that system (47) also reduces from a 12×12 system to a 6×6 system,

$$\begin{bmatrix} 2\lambda C_2 & -2\lambda S_2 & \Lambda C_1 & -\Lambda S_1 & 0 & 0 \\ -\Lambda S_2 & \Lambda C_2 & -2S_1 & 2C_1 & 0 & 0 \\ -C_4 & S_4 & -C_3 & S_3 & -S_4 & -S_3 \\ \lambda S_4 & -\lambda C_4 & S_3 & -C_3 & \lambda C_4 & C_3 \\ -2\lambda C_4 & 2\lambda S_4 & -\Lambda C_3 & \Lambda S_3 & -2\lambda\beta S_4 & -\Lambda\beta S_3 \\ \Lambda S_4 & -\Lambda C_4 & 2S_3 & -2C_3 & -\Lambda\beta C_4 & 2\beta C_3 \end{bmatrix} \begin{bmatrix} M_1^{(1)} \\ M_2^{(1)} \\ L_1^{(1)} \\ L_2^{(1)} \\ M_2^{(2)} \\ L_2^{(2)} \end{bmatrix} = \mathbf{0}_{6\times 1}, \tag{59}$$

where C_1, C_2, C_3, C_4, S_1, S_2, S_3, S_4 and Λ are again as given in (56). In this case the associated *barrelling buckling equation* shall be written as:

$$\Psi_B(\lambda, \eta, \beta, \alpha) = 0. \tag{60}$$

Both Ψ_F and Ψ_B are smooth functions of λ, η, β and α. For a given composite construction, both β and α are fixed. Then flexural and barrelling bifurcations are governed by the η-λ relation between the mode number and the load parameter that follows from (57) and (60), respectively.

Consider the flexural case. For a given triple (η, β, α) we then seek roots λ to (57). It is easily seen that

$$\Psi_F(1, \eta, \beta, \alpha) = 0,$$

since the final two columns in the coefficient matrix of (55) are then identical. Thus $\lambda = 1$ is always a solution to (57). However, since this corresponds to no end displacement and hence zero thrust, it is not of interest to us and so will not be considered further.

The complicated nature of (57) gives rise to formidable analytical difficulties. Consequently we have pursued a numerical investigation of this equation. Such an investigation indicates for fixed η, β, α that Ψ_F monotonically increases from $\Psi_F = -\infty$ at $\lambda = 0$ through $\Psi_F = 0$ at $\lambda = 1$ to some maximum value. Then Ψ_F subsequently is found to monotonically decrease, again passing through $\Psi_F = 0$. Thus in addition to the root $\lambda = 1$, a second root $\lambda > 1$ exists for equation (57). Moreover since $\lambda > 1$, these solutions only exist for compressive loads. We shall denote this root by

$$\lambda = \Phi_F(\eta, \beta, \alpha). \tag{61}$$

The barrelling case is similar, namely for all triples (β, η, α), $\lambda = 1$ is a root of (60). In addition we find that there always exists another root $\lambda > 1$ to the barrelling equation (60). We shall denote this root by

$$\lambda = \Phi_B(\eta, \beta, \alpha). \tag{62}$$

We have developed numerical routines, based on simple bisection, to determine the functions $\Phi_F(\eta, \beta, \alpha)$ and $\Phi_B(\eta, \beta, \alpha)$.

The failure stretch ratios are now defined as follows:

$$\left.\begin{aligned}\lambda_m^{\mathrm{F}} &= \Phi_{\mathrm{F}}(m\pi l_2/2l_1, \beta, \alpha)\\ \lambda_m^{\mathrm{B}} &= \Phi_{\mathrm{B}}(m\pi l_2/2l_1, \beta, \alpha)\end{aligned}\right\}, \quad m = 1, 2, 3, \ldots. \tag{63}$$

Once these failure stretch ratios are found, the corresponding failure thrusts are found from (28) and (29) using $\rho = \lambda^{-1/2}$. In particular, it is to be noted that the failure thrusts are ordered the same as the failure stretch ratios.

To find the ordering of the flexure failure stretch ratios for fixed values of β and α, one plots the sequence of points $(m\pi l_2/2l_1, \lambda_m^{\mathrm{F}})$ using (63). The *lowest* value of λ_m^{F} determines the *critical* mode number m for flexure as well as the critical flexure failure stretch ratio and hence the critical flexure failure thrust. The critical mode number m for barrelling as well as the critical barrelling failure stretch ratio and the critical barrelling failure thrust are found similarly.

For all of the noncomposite cases (53), the numerical method consistently gives the (η, λ) relation as found by Sawyers and Rivlin (1974, 1982) and displayed in Fig. 3. Notice in this case that Φ_{F} as a function of η is monotonically increasing from $\lambda = 1$ at $\eta = 0$ to $\lambda = 3.383\ldots$ as $\eta \to \infty$. Hence according to $(63)_1$ the flexural failure thrusts are ordered as follows:

$$0 < T_1^{\mathrm{F}} < T_2^{\mathrm{F}} < \cdots < T_m^{\mathrm{F}} < T_{m+1}^{\mathrm{F}} < \cdots \to T_\infty^{\mathrm{F}}, \tag{64}$$

where T_∞^{F} is found from (28) using the asymptotic value $\lambda = \rho^{-2} = 3.383\ldots$. Similarly for the noncomposite case, Φ_{B} as a function of η is monotonically decreasing from $\lambda = \infty$ at $\eta = 0$ to $\lambda = 3.383\ldots$ as $\eta \to \infty$. Hence according to $(63)_2$:

$$T_1^{\mathrm{B}} > T_2^{\mathrm{B}} > \cdots > T_m^{\mathrm{B}} > T_{m+1}^{\mathrm{B}} > \cdots \to T_\infty^{\mathrm{B}} > 0. \tag{65}$$

Finally, since both Φ_{F} and Φ_{B} have the same asymptote as $\eta \to \infty$, it follows that

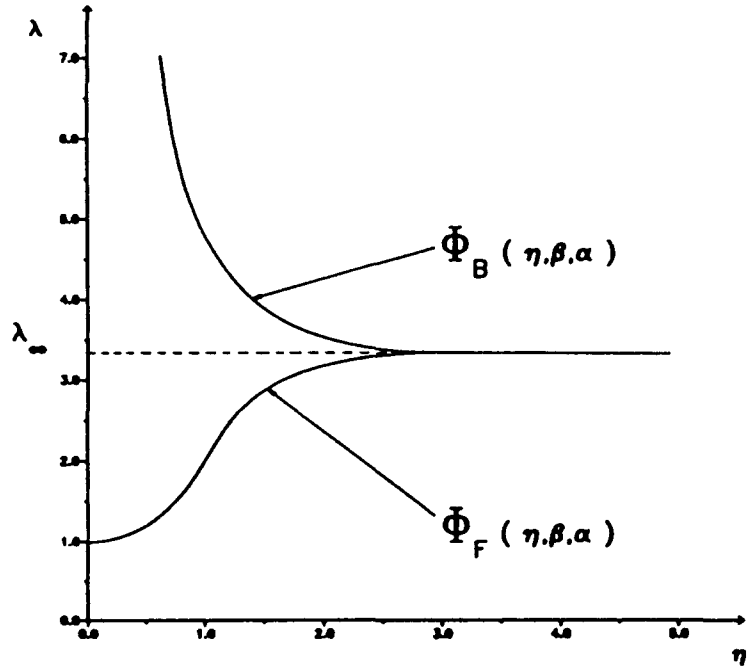

Fig. 3. The functions $\Phi_{\mathrm{F}}(\eta, \beta, \alpha)$ and $\Phi_{\mathrm{B}}(\eta, \beta, \alpha)$ for all (β, α) pairs corresponding to the noncomposite case given in (53). Here $\lambda_\infty \approx 3.383$.

$$T_{\lambda}^{F} = T_{\lambda}^{B} \equiv T_{\lambda}. \tag{66}$$

Physically T_{λ} gives rise to an instability which corresponds to a wrinkling failure. Combining (64)–(66) gives (1).

5. FLEXURE AND BARRELLING RESULTS FOR COMPOSITE CONFIGURATIONS

We find that the orderings (64), (65) and (1) given by Sawyers and Rivlin (1974, 1982) for noncomposite constructions, and confirmed in the previous section, will, for certain composite constructions, cease to hold. The ordering of the failure thrusts is determined by two factors: (i) the qualitative behavior of the functions $\Phi_F(\eta, \beta, \alpha)$ and $\Phi_B(\eta, \beta, \alpha)$ for fixed (β, α) as the mode parameter η is allowed to vary, and (ii) the spacing of the sequence of η values.

The qualitative behavior of the η-dependence can be characterized with respect to the parameter pair (β, α). The spacing of the values of η is then determined by the aspect ratio l_2/l_1. Thus the three parameters: ply stiffness ratio β, central ply volume fraction α, and aspect ratio l_2/l_1, completely determine the ordering of the failure thrusts for the problem at hand. Within this framework the present section is organized as follows. Beginning with the function $\Phi_F(\eta, \beta, \alpha)$ we document the possibilities for the qualitative behavior of the η-dependence. Then for each distinct qualitative behavior so obtained we examine the consequence of different possible spacings of η. We then follow a similar programme for the function $\Phi_B(\eta, \beta, \alpha)$. In this fashion we uncover the possible new ordering for the failure thrusts and correlate these new orderings with the associated composite constructions by means of the parameter pairs (β, α) and the aspect ratio l_2/l_1.

First of all, however, it will be expedient to demonstrate those qualitative behaviors that hold regardless of the pair (β, α). For all values of (β, α) we find that $\Phi_F(\eta, \beta, \alpha)$ is initially monotonically increasing from the value 1 at $\eta = 0$ and tends to an asymptotic value as $\eta \to \infty$. Similarly, for all values of (β, α) we find that $\Phi_B(\eta, \beta, \alpha)$ is initially monotonically decreasing from ∞ at $\eta = 0$ and tends to the same asymptotic value as $\eta \to \infty$. We shall denote this common asymptotic value as:

$$\lambda_{\infty}(\beta, \alpha) \equiv \lim_{\eta \to \infty} \Phi_F(\eta, \beta, \alpha) = \lim_{\eta \to \infty} \Phi_B(\eta, \beta, \alpha). \tag{67}$$

It is computed numerically in what follows by taking a cut-off value for η in (67). We also find that

$$\Phi_F(\eta, \beta, \alpha) < \Phi_B(\eta, \beta, \alpha) \tag{68}$$

for all finite $\eta > 0$. Thus (66) holds for all composite configurations where now $T_{\infty} = T_{\infty}(\beta, \alpha)$. In addition (68) yields

$$T_m^F < T_m^B, \quad m = 1, 2, 3, \ldots. \tag{69}$$

In particular, (69) indicates that *the critical flexure failure thrust is always less than the critical barrelling failure thrust. Thus the critical flexure failure thrust gives the first bifurcation for all pairs* (β, α) *and all aspect ratios* l_2/l_1 *within the class of plane strain bifurcations under consideration.*

We now turn to consider those qualitative behaviors for the η-dependence of the functions $\Phi_F(\eta, \beta, \alpha)$ and $\Phi_B(\eta, \beta, \alpha)$ which result in new orderings of the failure thrusts. The ordering (64) of flexural failure thrusts will continue to hold if $\Phi_F(\eta, \beta, \alpha)$ is monotonically increasing for all $\eta \geqslant 0$. Pairs (β, α) which give rise to $\Phi_F(\eta, \beta, \alpha)$ having this property will be said to belong to the set Γ_I^F. For example, we find that $(\beta, \alpha) = (0.5, 0.5) \in \Gamma_I^F$ (Fig. 4). Note in this case that $\lambda_{\infty} = 3.271\ldots$.

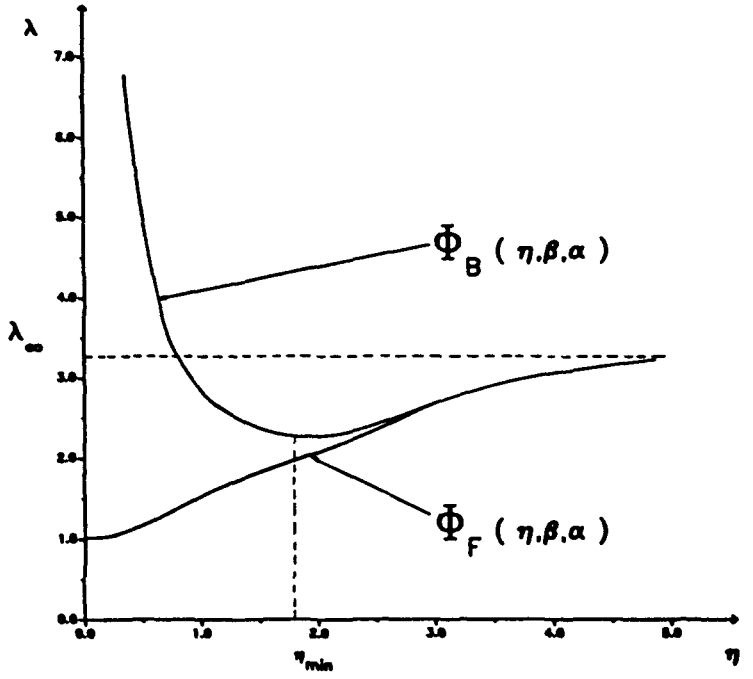

Fig. 4. The functions $\Phi_F(\eta, \beta, \alpha)$ and $\Phi_B(\eta, \beta, \alpha)$ for $(\beta, \alpha) = (0.5, 0.5)$. Here $(\beta, \alpha) \in \Gamma_I^F \cap \Gamma_{II}^B$ with $\lambda_\infty \approx 3.271$ and $\eta_{min} \approx 1.792$.

However, we find for certain pairs (β, α) that $\Phi_F(\eta, \beta, \alpha)$ is no longer monotonically increasing in η over the whole domain $\eta \geqslant 0$. In particular, it is sometimes found that $\Phi_F(\eta, \beta, \alpha)$ is monotonically increasing over a finite domain $0 \leqslant \eta < \eta_{max} = \eta_{max}(\beta, \alpha)$ but is subsequently monotonically decreasing to $\lambda_\infty(\beta, \alpha)$ for $\eta > \eta_{max}(\beta, \alpha)$. Pairs (β, α) which give rise to this behavior will be said to belong to the set Γ_{II}^F. For example, we find that $(2.0, 0.5) \in \Gamma_{II}^F$, in which case $\eta_{max} = 1.977\ldots$ and $\lambda_\infty = 3.439\ldots$ (Fig. 5).

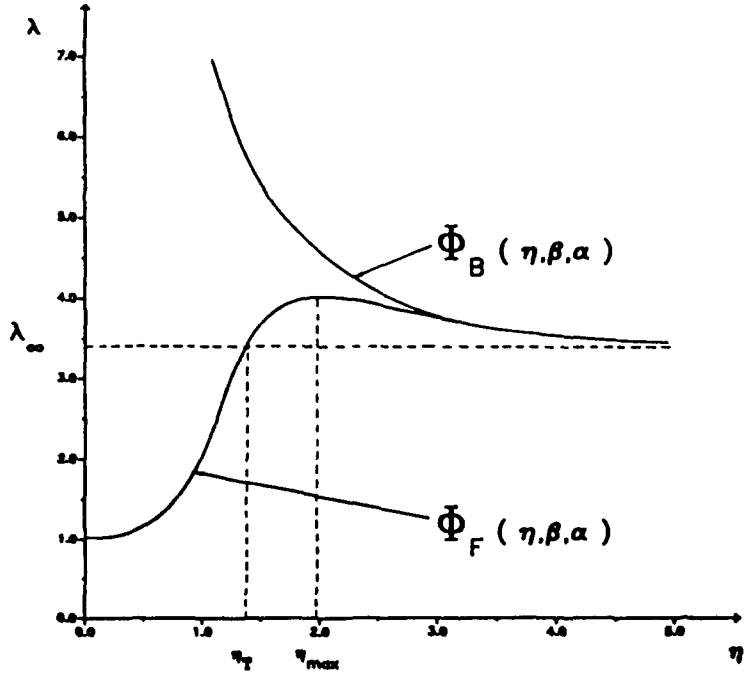

Fig. 5. The functions $\Phi_F(\eta, \beta, \alpha)$ and $\Phi_B(\eta, \beta, \alpha)$ for $(\beta, \alpha) = (2.0, 0.5)$. Here $(\beta, \alpha) \in \Gamma_{II}^F \cap \Gamma_I^B$ with $\lambda_\infty \approx 3.439$, $\eta_{max} \approx 1.977$ and $\eta_T \approx 1.392$.

Composite configurations for which $(\beta, \alpha) \in \Gamma_n^F$ give rise to flexure failure thrusts that no longer obey (64). To determine the ordering in such a case we note for $(\beta, \alpha) \in \Gamma_n^F$ that the equation

$$\Phi_F(\eta, \beta, \alpha) = \lambda_c(\beta, \alpha) \tag{70}$$

will have a unique finite root, which we shall denote by $\eta_T(\beta, \alpha)$, and that this root will obey

$$\eta_T(\beta, \alpha) < \eta_{max}(\beta, \alpha).$$

For example, referring to Fig. 5, we note that $\eta_T(2.0, 0.5) = 1.392\ldots < 1.977\ldots = \eta_{max}(2.0, 0.5)$. Recalling that the discrete values of the sequence of values of η is determined by l_2/l_1, it follows that, for a given aspect ratio l_2/l_1, one can then determine integers p, q such that

$$\begin{aligned} p\pi l_2/2l_1 < \eta_T \leqslant (p+1)\pi l_2/2l_1, \\ q\pi l_2/2l_1 \leqslant \eta_{max} < (q+1)\pi l_2/2l_1. \end{aligned} \tag{71}$$

It is clear that $0 \leqslant p \leqslant q$.

If $p > 0$ it follows that $\pi l_2/2l_1 < \eta_T$ so that T_1^F is the critical flexure failure thrust. In this event we may define the flexure failure thrust sequences

$$\begin{aligned} \mathcal{J}_1 &= \{T_1^F, \ldots, T_p^F\}, \\ \mathcal{J}_2 &= \{T_{p+1}^F, \ldots, T_q^F\}, \quad \text{(provided } p < q\text{)} \\ \mathcal{J}_3 &= \{T_{q+1}^F, \ldots \to T_c\}. \end{aligned}$$

The ordering of the flexure failure thrusts will now consist of $\mathcal{J}_1$ followed by an interlacing of $\mathcal{J}_2$ with a reverse ordering of the sequence $\mathcal{J}_3$.

On the other hand if $p = 0$, then $\pi l_2/2l_1 \geqslant \eta_T$. Assume for the moment that the inequality is strict. It then follows that T_c is the critical flexure failure thrust. In this event the sequence $\mathcal{J}_1$ is empty and the ordering of the flexure failure thrusts will consist of an interlacing of $\mathcal{J}_2$ with the reverse ordering of the sequence $\mathcal{J}_3$. It is to be emphasized in this interlacing that T_c will in this case lead the sequence of flexure failure thrusts.

In both cases $p = 0$ and $p > 0$ the thrust T_c is not an upper bound for the set of values T_m^L. Recall now that both the flexure failure thrusts and the barrelling failure thrusts cluster around T_c. Hence it may be concluded that some of the barrelling failure thrusts will be interlaced with some of the flexure failure thrusts.

Thus, if $(\beta, \alpha) \in \Gamma_n^L$, the flexure failure thrusts are interlaced with the barrelling failure thrusts regardless of aspect ratio l_2/l_1. The critical flexure failure thrust will, depending on the aspect ratio l_2/l_1, be either the $m = 1$ flexure failure or the $m = \infty$ wrinkling failure. The transition between the $m = 1$ flexure failure and the $m = \infty$ wrinkling failure occurs at the transition aspect ratio $l_2/l_1 = 2\eta_T/\pi$. At this transition aspect ratio $T_1^F = T_c^F$. Hence for a Γ_n^L plate which is sufficiently short in the direction of thrust [specifically $l_1 < l_2\pi/(2\eta_T)$], wrinkling is the critical flexural instability. However, for a Γ_n^F plate which is sufficiently long in the direction of thrust [specifically $l_1 > l_2\pi/(2\eta_T)$], the critical flexural instability is the $m = 1$ mode.

It is to be noted for $(\beta, \alpha) \in \Gamma_n^F$, that there exist infinitely many aspect ratios at which a flexure failure thrust from $\mathcal{J}_2$ will coincide with a flexure failure thrust from $\mathcal{J}_1$. To see this choose λ in the interval $\lambda_c < \lambda < \Phi_F(\eta_{max}, \beta, \alpha)$. There will exist two intersections of the horizontal line corresponding to this value of λ with the graph of $\Phi_F(\eta, \beta, \alpha)$. One intersection will occur in $\eta_T < \eta < \eta_{max}$ and the other will occur in $\eta > \eta_{max}$. Denote these intersection values of η by η_1 and η_2, respectively. The ratio η_2/η_1 can be made to take on any value greater than 1 by appropriately choosing λ in this procedure. If this ratio is a rational number it then follows that $\eta_2/\eta_1 = r/s$ for infinitely many integer pairs r and s. Choose one such integer pair, for example the case when r and s are coprime. Then the

aspect ratio $l_2/l_1 = 2\eta_1/(s\pi) = 2\eta_2/(r\pi)$ will yield $T_r^F = T_s^F$. Moreover, this construction will hold for each rational number greater than 1. We note that there is no possibility that a single flexure failure thrust could correspond to three or more flexure failure modes m whenever $(\beta, \alpha) \in \Gamma_{ii}^F$.

The regions Γ_i^F and Γ_{ii}^F in the semi-infinite strip

$$\Pi \equiv \{(\beta, \alpha) \mid \beta \geqslant 0, 0 \leqslant \alpha \leqslant 1\} \tag{72}$$

of possible (β, α) parameter pairs have been determined by means of an extensive numerical sampling procedure and are displayed in Fig. 6. Points to the right (left) of the vertical line segment $\beta = 1$ correspond to cases in which the central ply is composed of a material which is more (less) stiff than the material comprising the outer plies. Points above (below) the horizontal line $\alpha = 1/2$ correspond to cases in which the central ply comprises more (less) than half the construction. A conspicuous feature of Fig. 6 is the presence of a region Γ_{iii}^F corresponding to pairs (β, α) which belong to neither Γ_i^F nor Γ_{ii}^F. The meaning of this region will be discussed below. In Fig. 6 the points $(\beta, 0) \in \Gamma_i^F$, $(\beta, 1) \in \Gamma_i^F$ and $(1, \alpha) \in \Gamma_i^F$ by virtue of (53). However we find that pairs (β, α) very close to these values may in fact not belong to Γ_i^F. For example, we find that $(0.5, 0.99) \in \Gamma_{ii}^F$ and $(1.1, 0.5) \in \Gamma_{ii}^F$. The "threading" of the segment $\beta = 1$ through the "pass" created by regions Γ_{ii}^F and Γ_{iii}^F near $(\beta, \alpha) = (1.0, 0.9)$ is displayed in Fig. 7. The region boundaries in Figs 6 and 7 may shift as more refined numerical algorithms are developed.

The presence of Γ_{ii}^F so near the boundary $\alpha = 1$ for $0 < \beta < 1$ indicates that if the aspect ratio l_2/l_1 is sufficiently large then the addition of relatively thin and stiff outer layers can suppress the low wavelength flexure modes enough to lead to the dominance of the $m = \infty$ wrinkling instability. Since each pair $(\beta, \alpha) \in \Gamma_{ii}^F$ gives rise to an aspect ratio dependence upon the critical flexural instability, we display the value of $\eta_T(\beta, \alpha)$, which determines the transition aspect ratio, for representative pairs $(\beta, \alpha) \in \Gamma_{ii}^F$ in Table 1.

We now turn to consider the buckling behavior of composite constructions corresponding to parameter pairs $(\beta, \alpha) \in \Gamma_{iii}^F$. Each such pair (β, α) gives rise to a function $\Phi_F(\eta, \beta, \alpha)$ which contains both internal maxima and internal minima as η varies from 0 to ∞. The ordering of the flexure failure thrusts for composite configurations in which $(\beta, \alpha) \in \Gamma_{iii}^F$ may in fact be quite complicated. First of all it is to be noted that (64) might still hold.

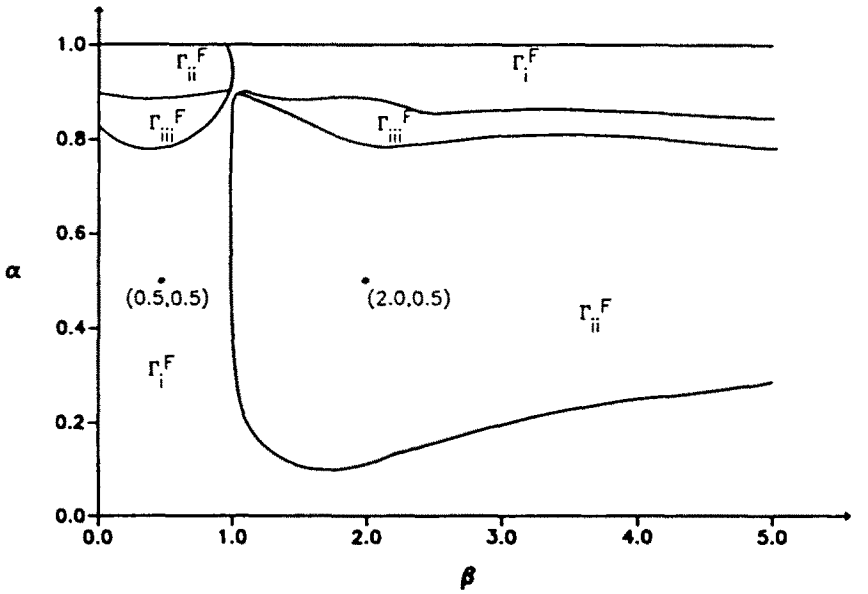

Fig. 6. Flexure failure behavior as represented in the semi-infinite strip $0 < \alpha = R'/l_2 < 1$, $0 < \beta = \mu^{(III)}/\mu^{(I)}$. The region types for each shade are as displayed. The two points shown correspond to the parameter pairs associated with Figs 4 and 5. Although it is not always obvious from this diagram, the parameter pairs obeying (53) are in the region Γ_i^F.

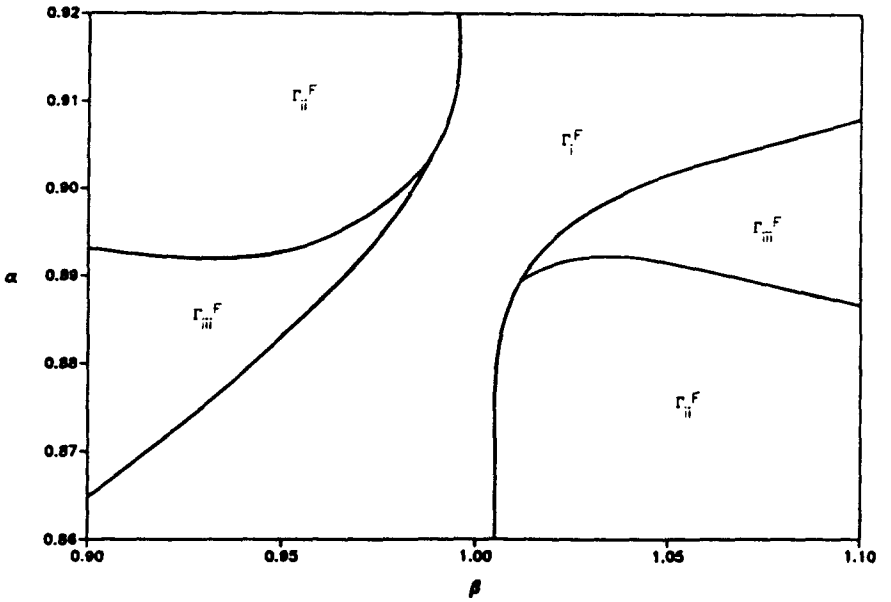

Fig. 7. Magnified view of Fig. 6 near $(\beta, \alpha) = (1.0, 0.9)$. The points on $\beta = 1$ are ensured to lie on Γ_i^+ by virtue of (53).

Specifically, if the number of internal maxima is finite and equal to the number of internal minima, then the asymptotic value λ_∞ will be approached from below and consequently (64) will continue to hold for sufficiently large aspect ratios l_2/l_1. However, for each $(\beta, \alpha) \in \Gamma_{iii}^+$ it is also clear that there will exist certain aspect ratios such that (64) will not hold. In particular, for each $(\beta, \alpha) \in \Gamma_{iii}^+$ there will exist infinitely many aspect ratios such that certain flexure failure thrusts will correspond to two distinct flexure modes m by the same argument used for $(\beta, \alpha) \in \Gamma_{ii}^+$. Finally, the possibility of a single flexure failure thrust corresponding to three or more flexure modes m remains a possibility whenever $(\beta, \alpha) \in \Gamma_{iii}^+$.

We now turn to consider the barrelling failure thrusts. The ordering (65) of barrelling failure thrusts will continue to hold if $\Phi_B(\eta, \beta, \alpha)$ is monotonically decreasing in η for all $\eta \geqslant 0$. Pairs (β, α) which give rise to $\Phi_B(\eta, \beta, \alpha)$ having this property will be said to belong to the set Γ_i^B. For example, $(2.0, 0.5) \in \Gamma_i^B$ (Fig. 5).

On the other hand if $\Phi_B(\eta, \beta, \alpha)$ is found to be monotonically decreasing over an interval $0 \leqslant \eta < \eta_{\min} = \eta_{\min}(\beta, \alpha)$ and is subsequently monotonically increasing for $\eta > \eta_{\min}(\beta, \alpha)$, then we shall say that $(\beta, \alpha) \in \Gamma_{ii}^B$. For example, $(0.5, 0.5) \in \Gamma_{ii}^B$ (Fig. 4). Finally,

Table 1. Value of $\eta_T(\beta, \alpha)$, which determines the transition aspect ratio, for representative pairs $(\beta, \alpha) \in \Gamma_{ii}^+$. For $l_2/l_1 < 2\eta_T\pi$, the critical instability is the $m = 1$ flexure mode, while for $l_2/l_1 > 2\eta_T\pi$ the critical instability is the $m = \infty$ wrinkling mode

	β=0.1	0.2	0.5	0.8	0.9	1.0	1.1	1.5	2	2.5	3	4	β=5
α=1	/	/	/	/	/	/	/	/	/	/	/	/	/
.99	0.974	1.236	1.948	2.810	3.602	/	/	/	/	/	/	/	/
.95	0.593	0.780	1.147	1.692	2.125	/	/	/	/	/	/	/	/
.9	0.555	0.711	1.070	1.653	2.166	/	/	/	/	/	/	/	/
.8	/	/	/	/	/	/	2.264	1.841	1.858	2.102	2.274	2.798	/
.7	/	/	/	/	/	/	1.862	1.383	1.410	1.439	1.599	1.726	1.912
.6	/	/	/	/	/	/	1.818	1.333	1.349	1.395	1.554	1.698	1.877
.5	/	/	/	/	/	/	1.951	1.347	1.392	1.497	1.675	1.965	2.147
.4	/	/	/	/	/	/	2.410	1.483	1.546	1.729	1.962	2.322	2.616
.3	/	/	/	/	/	/	3.186	1.764	1.889	2.196	2.536	3.060	3.865
.2	/	/	/	/	/	/	4.753	2.465	2.711	3.228	3.829	4.784	5.826
.1	/	/	/	/	/	/	/	4.857	5.065	5.903	6.898	/	/
α=0	/	/	/	/	/	/	/	/	/	/	/	/	/

if (β, α) belongs to neither Γ_i^B nor Γ_{ii}^B then we shall say that $(\beta, \alpha) \in \Gamma_{iii}^B$. Clearly $(\beta, \alpha) \in \Gamma_{iii}^B$ implies that $\Phi_B(\eta, \beta, \alpha)$ has an internal maximum.

For $(\beta, \alpha) \in \Gamma_{ii}^B$, relation (65) will no longer hold. Specifically, T_x can no longer be the critical barrelling failure thrust. In fact, the critical barrelling failure thrust can be made to correspond to *any* mode number $m < \infty$ by, for example, taking an aspect ratio $l_2/l_1 = 2\eta_{min}(\beta, \alpha)\ (m\pi)$. Coincidence of two failure barrelling thrusts is also a possibility whenever $(\beta, \alpha) \in \Gamma_{ii}^B$. In fact for consecutive integers m and $m+1$, if $T_m^B = T_{m+1}^B$ then this common value of barrelling failure thrust must of necessity be the critical barrelling failure thrust. Moreover, it can be shown that there exists a unique aspect ratio such that $T_m^B = T_{m+1}^B$ for any integer m. Finally, it is to be noted that interlacing of the flexural and barrelling buckling loads will occur regardless of aspect ratio l_2/l_1 if $(\beta, \alpha) \in \Gamma_{ii}^B$.

If $(\beta, \alpha) \in \Gamma_{iii}^B$, then the ordering of the barrelling failure thrusts is complicated by the precise placement of the internal maxima and minima of $\Phi_B(\eta, \beta, \alpha)$. In fact, phenomena paralleling the possibilities outlined previously for Γ_{iii}^F pertain also to Γ_{iii}^B.

The partitioning of Π into regions Γ_i^B, Γ_{ii}^B and Γ_{iii}^B is displayed in Fig. 8. Note that the boundary of the region Γ_{ii}^B is at certain points quite close to the pairs (β, α) corresponding to the noncomposite case (53). The presence of Γ_{ii}^B so near the boundary $\alpha = 1$ for $\beta > 1$ indicates that a plate which includes relatively thin and flexible outer layers can be "tuned" to any desired critical barrelling mode by appropriately selecting the aspect ratio l_2/l_1. For such a result to be of significant practical interest, however, it would seem that it would be necessary to devise a method to suppress the preceding flexure modes.

Since the interlacing of the flexural and barrelling failure modes is an intriguing result, it would be useful to further characterize this behavior with respect to β, α and l_2/l_1. For a given pair (β, α), interlacing can be made to occur for at least one l_2/l_1 if for any value of η either $\Phi_I(\eta, \beta, \alpha) > \lambda_1$ or $\Phi_{II}(\eta, \beta, \alpha) < \lambda_1$. Furthermore interlacing is ensured for all l_2/l_1 if either $\Phi_I(\eta, \beta, \alpha)$ approaches λ_1 from above as $\eta \to \infty$ or if $\Phi_{II}(\eta, \beta, \alpha)$ approaches λ_1 from below as $\eta \to \infty$. One or the other such asymptotic behaviors giving rise to interlacing for all l_2/l_1 will occur if either $(\beta, \alpha) \in \Gamma_{ii}^I$ or $(\beta, \alpha) \in \Gamma_{ii}^{II}$. In addition, an asymptotic behavior that ensures interlacing could also occur if $(\beta, \alpha) \in \Gamma_{iii}^I \cup \Gamma_{iii}^{II}$; however, for such points this asymptotic behavior may be extremely sensitive to small changes in (β, α) and hence difficult to determine. Even so, it is interesting to note from Figs 6 and 8 that points $(\beta, \alpha) \in \Gamma_{ii}^I \cup \Gamma_{ii}^{II}$ comprise the major portion of the strip Π for both $\beta > 1$ and $\beta < 1$. Thus, from

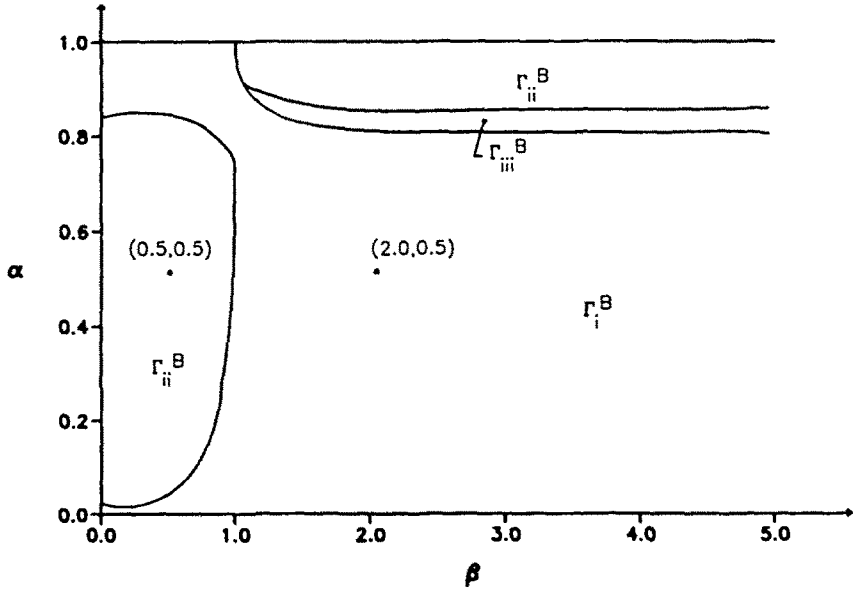

Fig. 8. Barrelling failure behavior as represented in the semi-infinite strip $0 < \alpha = R/l_2 < 1$, $0 < \beta = \mu^{(II)}/\mu^{(I)}$. The region types for each shade are as displayed. The two points shown correspond to the parameter pairs associated with Figs 4 and 5. Although it is not always obvious from this diagram, the parameter pairs obeying (53) are in the region Γ_i^B.

this point of view, interlacing is not at all unusual both when the stiffer material comprises the outer layers ($\beta < 1$, e.g. Fig. 4), and when the stiffer material comprises the central ply ($\beta > 1$, e.g. Fig. 5).

It is also interesting to classify the points (β, α) with respect to satisfaction of eqns (64) and (65). There are three possibilities. First, it may be that both (64) and (65)—and thus (1)—hold for all aspect ratios l_2/l_1. In this case we shall say that $(\beta, \alpha) \in \Xi_1$. For this to occur the pair (β, α) must belong to *both* Γ_i^F *and* Γ_i^B. Second, it may be that there is at least one aspect ratio l_2/l_1 that will result in both (64) and (65) being violated. For this to occur the pair (β, α) must belong to *neither* Γ_i^F *nor* Γ_i^B. In this case we shall say that $(\beta, \alpha) \in \Xi_2$. Finally, it may be that for each aspect ratio l_2/l_1 either (64) or (65) holds, but that there is also at least one aspect ratio l_2/l_1 for which one of these relations is violated. This will occur for the remaining case in which (β, α) belongs to *either* Γ_i^F *or* Γ_i^B, *but not both*. In this case we shall say that $(\beta, \alpha) \in \Xi_3$. Summarizing then these definitions,

$$\begin{aligned}
\Xi_1 &= \Gamma_i^F \cap \Gamma_i^B, \\
\Xi_2 &= (\Gamma_{ii}^F \cup \Gamma_{iii}^F) \cap (\Gamma_{ii}^B \cup \Gamma_{iii}^B), \\
\Xi_3 &= (\Gamma_i^F \cap (\Gamma_{ii}^B \cup \Gamma_{iii}^B)) \cup (\Gamma_i^B \cap (\Gamma_{ii}^F \cup \Gamma_{iii}^F)).
\end{aligned} \tag{73}$$

One can determine these regions on the basis of Figs 6 and 8, the result of which is given in Fig. 9. This figure indicates that Ξ_1 is confined to a simply connected region containing pairs (β, α) corresponding to the noncomposite case (53). Thus, in this sense, *the composite constructions under consideration must be "close" to a noncomposite construction if* (1) *is to hold*. Figure 9 also indicates that the region Ξ_1 comprises the majority of the semi-infinite strip II. In particular, the (β, α) pairs (0.5, 0.5) and (2.0, 0.5), associated with Figs 4 and 5 respectively, are each a member of Ξ_1. The region Ξ_2, on the other hand, comprises the least area within the semi-infinite strip II. For pairs $(\beta, \alpha) \in \Xi_2$ both $\Phi_I(\eta, \beta, \alpha)$ and $\Phi_{II}(\eta, \beta, \alpha)$ display nonmonotone behavior as, for example, shown in Fig. 10 for the point $(\beta, \alpha) = (0.5, 0.8)$. Finally, it is to be noted from Fig. 9 that the (β, α) classification is far more sensitive near $\alpha = 1$ than it is near $\alpha = 0$. This confirms our intuition as to the effect that placement of thin "stiffeners" (or even "looseners") would have in a much thicker homogeneous plate;

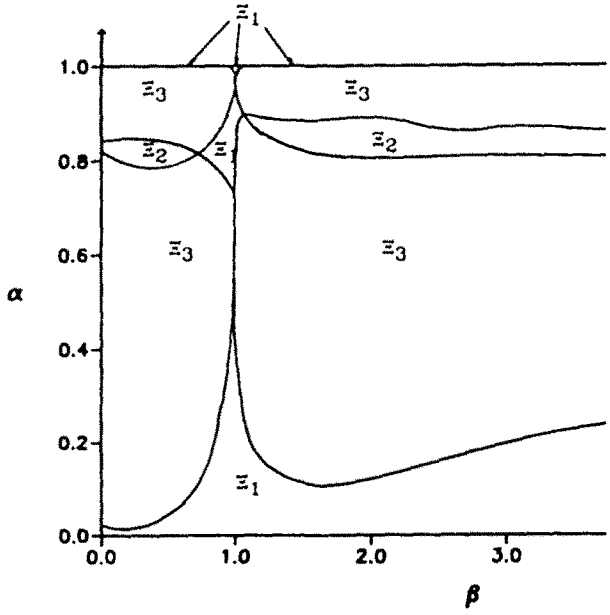

Fig. 9. The partitioning of the semi-infinite strip $0 < \alpha = R/l_2 < 1$, $0 < \beta = \mu^{(II)}/\mu^{(I)}$ into the regions Ξ_1, Ξ_2 and Ξ_3. The ordering (1) is ensured only for $(\beta, \alpha) \in \Xi_1$. For $(\beta, \alpha) \in \Xi_2 \cup \Xi_3$ the ordering which replaces (1) is dependent on the aspect ratio l_2/l_1. Although it is not always obvious from this diagram, the parameter pairs obeying (53) are in the region Ξ_1.

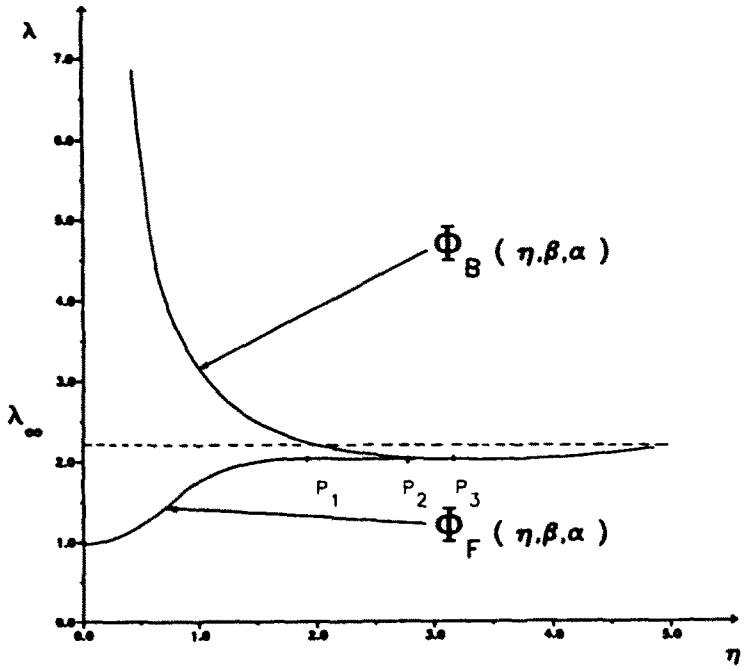

Fig. 10. The function $\Phi_F(\eta, \beta, \alpha)$ and $\Phi_B(\eta, \beta, \alpha)$ for $(\beta, \alpha) = (0.5, 0.8)$. Here $(\beta, \alpha) \in \Gamma_u^{II} \cap \Gamma_m^{I}$. A maximum of the function $\Phi_F(\eta, \beta, \alpha)$ occurs at $(\eta, \lambda) = P_1 \approx (1.925, 2.030)$ and a minimum of the function occurs at $(\eta, \lambda) = P_2 \approx (2.811, 2.021)$. A single minimum in the function $\Phi_B(\eta, \beta, \alpha)$ occurs at $(\eta, \lambda) = P_3 \approx (3.197, 2.041)$.

namely that the addition of thin plies on the external X_2 faces of the plate would have a more pronounced effect on the buckling behavior than would the insertion of a single double thickness ply on the plate's midplane. Thus it is found that burying a very thin ply at the center of a plate will mask its effect upon altering the order of the failure thrusts. More general issues related to the modification of buckling behavior by means of ply placement are currently under investigation.

Acknowledgement—This work was supported by the Composite Materials and Structures Center, Michigan State University, under the REF program.

REFERENCES

Davies, P. J. (1989). Buckling and barrelling instabilities in finite elasticity. *J. Elast.* **21**, 147–192.

Horgan, C. O. and Pence T. J. (1989). Void nucleation in tensile dead-loading of a composite incompressible nonlinearly elastic sphere. *J. Elast.* **21**, 61–82.

Sawyers, K. N. and Rivlin, R. S. (1974). Bifurcation condition for a thick elastic plate under thrust. *Int. J. Solids Structures* **10**, 483–501.

Sawyers, K. N. and Rivlin, R. S. (1982). Stability of a thick elastic plate under thrust. *J. Elast.* **12**, 101–124.

Simpson, H. C. and Spector, S. J. (1984). On barrelling for a special material in finite elasticity. *Q. Appl. Math.* **42**, 99–111.

APPENDIX

Submatrices $\mathbf{J}_{mn}$ in (51):

$$\mathbf{J}_{12} = \mathbf{J}_{21} = \mathbf{J}_{31} = \mathbf{0}_{4\times 4},$$

$$\mathbf{J}_{11} = \begin{bmatrix} 2\lambda C_2 & -2\lambda S_2 & \Lambda C_1 & -\Lambda S_1 \\ -\Lambda S_2 & \Lambda C_2 & -2S_1 & 2C_1 \\ 0 & 0 & 0 & 0 \\ 0 & 0 & 0 & 0 \end{bmatrix}.$$

$$\mathbf{J}_{11} = \begin{bmatrix} 0 & 0 & 0 & 0 \\ 0 & 0 & 0 & 0 \\ 2\lambda C_2 & 2\lambda S_2 & \Lambda C_1 & \Lambda S_1 \\ \Lambda S_2 & \Lambda C_2 & 2S_1 & 2C_1 \end{bmatrix},$$

$$\mathbf{J}_{21} = \begin{bmatrix} -C_4 & S_4 & -C_3 & S_3 \\ \lambda S_4 & -\lambda C_4 & S_3 & -C_3 \\ -2\lambda C_4 & 2\lambda S_4 & -\Lambda C_3 & \Lambda S_3 \\ \Lambda S_4 & -\Lambda C_4 & 2S_3 & -2C_3 \end{bmatrix},$$

$$\mathbf{J}_{22} = \begin{bmatrix} C_4 & -S_4 & C_3 & -S_3 \\ -\lambda S_4 & \lambda C_4 & -S_3 & C_3 \\ 2\beta\lambda C_4 & -2\beta\lambda S_4 & \beta\Lambda C_3 & -\beta\Lambda S_3 \\ -\beta\Lambda S_4 & \beta\Lambda C_4 & -2\beta S_3 & 2\beta C_3 \end{bmatrix},$$

$$\mathbf{J}_{12} = \begin{bmatrix} -C_4 & -S_4 & -C_3 & -S_3 \\ -\lambda S_4 & -\lambda C_4 & -S_3 & -C_3 \\ -2\beta\lambda C_4 & -2\beta\lambda S_4 & -\beta\Lambda C_3 & -\beta\Lambda S_3 \\ -\beta\Lambda S_4 & -\beta\Lambda C_4 & -2\beta S_3 & -2\beta C_3 \end{bmatrix},$$

$$\mathbf{J}_{11} = \begin{bmatrix} C_4 & S_4 & C_3 & S_3 \\ \lambda S_4 & \lambda C_4 & S_3 & C_3 \\ 2\lambda C_4 & 2\lambda S_4 & \Lambda C_3 & \Lambda S_3 \\ \Lambda S_4 & \Lambda C_4 & 2S_3 & 2C_3 \end{bmatrix},$$

where

$$C_1 = \cosh(\eta), \quad C_2 = \cosh(\lambda\eta), \quad C_3 = \cosh(\eta\alpha), \quad C_4 = \cosh(\lambda\eta\alpha),$$
$$S_1 = \sinh(\eta), \quad S_2 = \sinh(\lambda\eta), \quad S_3 = \sinh(\eta\alpha), \quad S_4 = \sinh(\lambda\eta\alpha),$$
$$\Lambda = (\lambda + 1/\lambda).$$